Available online at www.sciencedirect.com
ScienceDirect
Journal of Sound and Vibration 322 (2009) 554–563
JOURNAL OF SOUND AND VIBRATION
www.elsevier.com/locate/jsvi

Transition from normal to local modes in an elastic beam supported by nonlinear springs

V.N. Pilipchuk[1]

Department of Theoretical and Applied Mechanics, The National University, Dnepropetrovsk 49050, Ukraine

Accepted 16 September 2008
The peer review of this article was organised by the Guest Editor
Available online 31 October 2008

Abstract

The transient mode localization phenomenon is considered in a mechanical model combining a simply supported beam and transverse nonlinear springs with hardening characteristics. Two different approaches to the model reduction, such as normal and local mode representations for the beam's center line, are discussed. It is concluded that the local mode discretization brings advantages for the transient localization analysis. Based on the specific coordinate transformations and the idea of averaging, explicit equations describing the energy exchange between the local modes and the corresponding localization conditions are obtained. It was shown that when the energy is slowly pumped into the system then, at some point, the energy equipartition around the system suddenly breaks and one of the local modes becomes the dominant energy receiver. The phenomenon is interpreted in terms of the related phase-plane diagram which shows qualitative changes near the image of the out-of-phase mode as the total energy of the system has reached its critical level. A simple closed form expression is obtained for the corresponding critical time estimate.

1. Introduction

The concept of nonlinear local modes was introduced in molecular physics several decades ago; see for instance Refs. [1,2] and the original references therein. Different interpretations and literature overviews from the standpoints of theoretical mechanics and mechanical engineering can be found in Refs. [3,4].

The nonlinear localization phenomenon develops at high-energy levels whereas the low-energy dynamics represents a superposition of normal modes usually with few dominant modes. It is shown below that, as the total energy of the system slowly increases then, at some point, a spontaneous dynamic transition from normal to local modes may occur. In order to describe such transitions and determine the corresponding critical conditions, an analytical tool is introduced through specific coordinate transformations and the idea of averaging. More introductory comments and references are given in the main text after the related equations have been derived.

E-mail addresses: valery.pilipchuk@yahoo.com, valery.pilipchuk@sbcglobal.net (V.N. Pilipchuk).
[1]Current work address: R&D, GM Technical Center, Warren, MI, USA.

0022-460X/$ - see front matter
doi:10.1016/j.jsv.2008.09.022

Finally, we note that the major complicating factor of such transient analyses has a geometrical nature. Indeed, the transition from normal to local modes is associated with a switch from one natural basis to another. This issue is discussed in detail in Section 3 of this paper. Then Sections 4 and 5 describe the analytical stages of the dynamic analysis. Below, Section 2 introduces the mechanical model chosen for illustration.

2. System description

The model under investigation represents a simply supported elastic beam of length l with two masses attached to the beam and connected to the base by nonlinear springs; see Fig. 1. The corresponding differential equation of motion and boundary conditions are, respectively,

$$\rho A \frac{\partial^2 w}{\partial t^2} + EI \frac{\partial^4 w}{\partial y^4} = f_1(t)\delta(y - y_1) + f_2(t)\delta(y - y_2) \tag{1}$$

and

$$w(t,y)|_{y=0,l} = 0, \quad \left.\frac{\partial^2 w(t,y)}{\partial y^2}\right|_{y=0,l} = 0 \tag{2}$$

where

$$f_i(t) = -f[w(t,y_i)] - c\frac{\partial w(t,y_i)}{\partial t} - m\frac{\partial^2 w(t,y_i)}{\partial t^2}, \quad i = 1,2 \tag{3}$$

are transverse forces applied to the beam from masses attached at the two points $y = y_{1,2}$.

It will be assumed that the model is perfectly symmetric with respect to $y = l/2$ so that the springs are attached at points

$$y_1 = l/3 \quad \text{and} \quad y_2 = 2l/3 \tag{4}$$

Below we consider the case of the hardening restoring force characteristics of the springs and show that, under appropriate conditions, a slow energy in-flow leads to the localization of vibration modes. As a result,

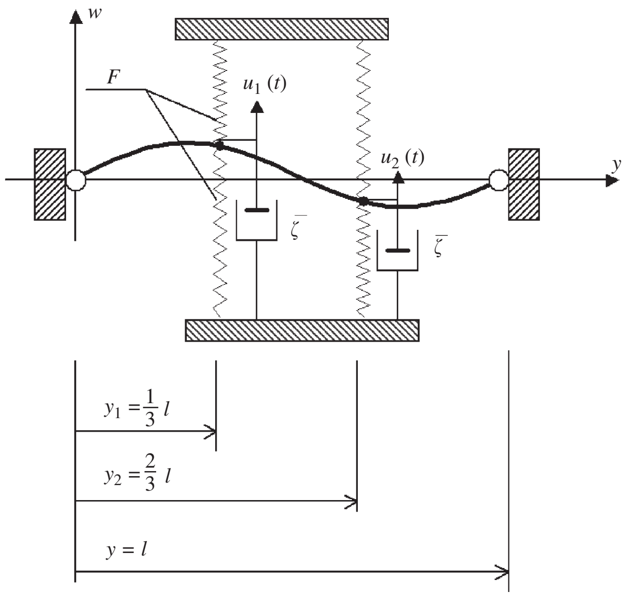

Fig. 1. The mechanical model admitting both normal and local mode motions; all the springs have hardening restoring force characteristics.

the system energy is spontaneously shifted to either the left or right side of the beam—the symmetry break. The adiabatically ‘slow’ energy increase means that the energy source has a minor or no direct effect on the mode shapes. For simulation purposes, such an energy in-flow is provided by the assumption that the viscous damping coefficient c is sufficiently small and negative; the physical basis for such an assumption was discussed in previous work [5]. This remark, which is substantiated below by the corresponding numerical values of the parameters, is important to follow, otherwise the phenomenon, which is the focus of this paper, may not be developed. In contrast, the dissipation ($c>0$) can lead to a spontaneous dynamic transition from local to normal modes, when the total energy reaches its sub-critical level.

Note that the presence of Dirac δ-functions in Eq. (1) requires a generalized interpretation of the differential equation of motion in terms of distributions [6]. The corresponding compliance is provided by further model reduction based on the Bubnov–Galerkin approach, which actually switches from the point-wise to integral interpretation of equations.

3. Normal and local mode coordinates

Normal mode coordinates. Let us evaluate two possible ways to discretizing model (1). In this paper, the reduced-order case of two degrees-of-freedom is considered, when the conventional normal mode representation for the boundary value problem (1) and (2) is

$$w(t,y) = W_1(t)\sin\frac{\pi y}{l} + W_2(t)\sin\frac{2\pi y}{l} \tag{5}$$

Substituting Eq. (5) in Eq. (1) and applying the standard Bubnov–Galerkin procedure, gives, after dropping the time arguments,

$$\ddot{W}_1 + \bar{\zeta}\dot{W}_1 + \lambda^2 W_1 + F(W_1 + W_2) + F(W_1 - W_2) = 0$$

$$\ddot{W}_2 + \bar{\zeta}\dot{W}_2 + 16\lambda^2 W_2 + F(W_1 + W_2) - F(W_1 - W_2) = 0 \tag{6}$$

where

$$\bar{\zeta} = \frac{3c}{3m + Al\rho}, \quad \lambda^2 = \frac{\pi^4 EI}{l^3(3m + Al\rho)} \tag{7}$$

and

$$F(z) = \frac{\sqrt{3}}{3m + Al\rho} f\left(\frac{\sqrt{3}}{2}z\right) \tag{8}$$

are constant parameters and a re-scaled restoring force function, respectively.

Eqs. (6) are decoupled in the linear terms related to the elastic beam center line, whereas the modal coupling is due to the spring nonlinearities included in $F(z)$.

Local mode coordinates. Alternatively, the model can be discretized by introducing the ‘local mode’ coordinates determined by the spring locations

$$u_i(t) = w(t, y_i), \quad i = 1, 2 \tag{9}$$

Taking into account Eqs. (4) and (5), and substitution in Eq. (9) reveals simple links between the normal and local coordinates as

$$u_1 = \frac{\sqrt{3}}{2}(W_1 + W_2), \quad u_2 = \frac{\sqrt{3}}{2}(W_1 - W_2) \tag{10}$$

or, inversely,

$$W_1 = \frac{\sqrt{3}}{3}(u_1 + u_2), \quad W_2 = \frac{\sqrt{3}}{3}(u_1 - u_2) \tag{11}$$

Substituting Eq. (11) in Eq. (5) gives the ‘local mode expansion’ for the beam’s center line

$$w(t,y) = u_1(t)\psi_1\left(\frac{\pi y}{l}\right) + u_2(t)\psi_2\left(\frac{\pi y}{l}\right) \tag{12}$$

where the local mode shape functions are

$$\begin{bmatrix} \psi_1(x) \\ \psi_2(x) \end{bmatrix} = \frac{\sqrt{3}}{3}\begin{bmatrix} 1 & 1 \\ 1 & -1 \end{bmatrix}\begin{bmatrix} \sin x \\ \sin 2x \end{bmatrix} \tag{13}$$

Both normal and local mode shape functions are shown in Figs. 2 and 3, respectively. Transformation (13) can be generalized for a greater number of modes. Note that functions (13) satisfy the following orthogonality condition:

$$\int_0^\pi \psi_i(x)\psi_j(x)\,\mathrm{d}x = \frac{\pi}{3}\delta_{ij} \tag{14}$$

where δ_{ij} is the Kronecker symbol.

However, the differential equations of motion for $u_1(t)$ and $u_2(t)$ are obtained directly by substituting Eq. (11) in Eq. (6) and making obvious algebraic manipulations that gives

$$\ddot{u}_1 + \bar{\zeta}\dot{u}_1 + (\lambda^2/2)(17u_1 - 15u_2) + \sqrt{3}F(2u_1/\sqrt{3}) = 0$$

$$\ddot{u}_2 + \bar{\zeta}\dot{u}_2 - (\lambda^2/2)(15u_1 - 17u_2) + \sqrt{3}F(2u_2/\sqrt{3}) = 0 \tag{15}$$

This kind of discretization seems to be similar to that given by the finite element approaches.

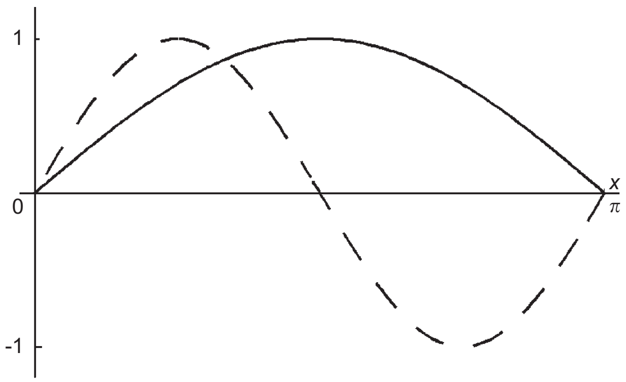

Fig. 2. Normal mode shape functions; here and below dashed lines correspond to second mode.

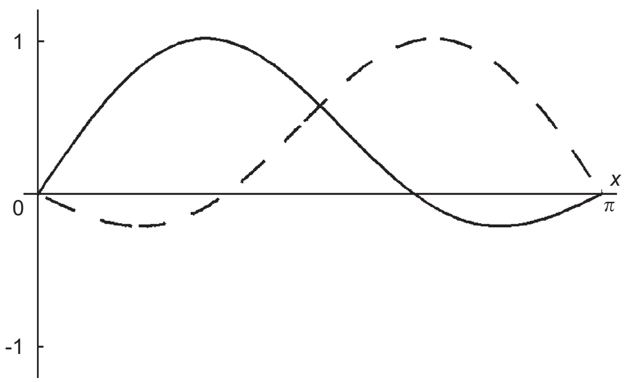

Fig. 3. Local mode shape functions.

Further, Eq. (15) are represented as a set of first-order equations

$$\dot{u}_1 = v_1$$
$$\dot{u}_2 = v_2$$
$$\dot{v}_1 = -\omega^2 u_1 + \varepsilon[\omega^2 u_2 - \zeta v_1 - p(u_1)]$$
$$\dot{v}_2 = -\omega^2 u_2 + \varepsilon[\omega^2 u_1 - \zeta v_2 - p(u_2)] \tag{16}$$

where

$$\omega = \sqrt{2k + \frac{17}{2}\lambda^2}, \quad k = F'(0), \quad \varepsilon = \frac{15}{2}\left(\frac{\lambda}{\omega}\right)^2, \quad \zeta = \frac{\bar{\zeta}}{\varepsilon}$$

and

$$p(u_i) = \frac{\sqrt{3}}{\varepsilon}\left[F\left(\frac{2\sqrt{3}}{3}u_i\right) - \frac{2\sqrt{3}}{3}ku_i\right] = \beta u_i^3$$

are new constant parameters and the nonlinear component of the spring characteristic; it is assumed that the damping coefficient and the nonlinear component are small enough to provide the order of magnitude $\zeta = O(1)$ and $p(u_i) = O(1)$.

For calculation purposes, the spring characteristic is taken in the form $F(u) = u + (4/3)u^3$ which brings the nonlinearity parameter β to the form

$$\beta = \frac{64\omega^2}{135\lambda^2} \tag{17}$$

Eqs. (15), and analogously Eq. (16), possess advantages for transient analysis because the corresponding linearized system has the same natural frequencies and the nonlinear components are decoupled. As a result, the one-frequency perturbation tool becomes applicable. The corresponding amplitude-phase variables are introduced as follows:

$$u_i = \alpha_i(t)\cos[\omega t + \delta_i(t)]$$
$$v_i = -\omega\alpha_i(t)\sin[\omega t + \delta_i(t)] \quad (i = 1, 2) \tag{18}$$

Substituting Eq. (18) in Eq. (16) and applying the averaging procedure with respect to the fast phase $z = \omega t$, gives

$$\dot{\alpha}_1 = -\frac{\varepsilon}{2}[\zeta\alpha_1 + \omega\alpha_2\sin(\delta_1 - \delta_2)]$$
$$\dot{\alpha}_2 = -\frac{\varepsilon}{2}[\zeta\alpha_2 - \omega\alpha_1\sin(\delta_1 - \delta_2)]$$
$$\dot{\delta}_1 = -\frac{\varepsilon\omega}{2}\frac{\alpha_2}{\alpha_1}\cos(\delta_1 - \delta_2) + \frac{3\varepsilon\beta}{8\omega}\alpha_1^2$$
$$\dot{\delta}_2 = -\frac{\varepsilon\omega}{2}\frac{\alpha_1}{\alpha_2}\cos(\delta_1 - \delta_2) + \frac{3\varepsilon\beta}{8\omega}\alpha_2^2 \tag{19}$$

The result of the work of Ref. [5] as well as further analysis show that the localization may occur as the system vibrates in the out-of-phase mode, $u_1(t) \equiv -u_2(t)$. In order to investigate the dynamics near the out-of-phase vibration mode, let us introduce three new variables s, ρ and θ,

$$\alpha_1 = -s(t) + \rho(t)$$
$$\alpha_2 = s(t) + \rho(t)$$
$$\delta_2 = \delta_1 + \Delta(t) \tag{20}$$

where s and ρ characterize the amplitudes of the out-of-phase and in-phase modes, respectively, and Δ is a phase shift between the local modes so that the variables ρ and Δ describe small deviations from the out-of-phase mode.

Substituting Eq. (20) in Eq. (19), linearizing the result with respect to ρ and Δ and then eliminating the phase variable Δ, gives

$$\ddot{\rho} + \varepsilon\zeta\dot{\rho} + \varepsilon^2(\omega^2 + \tfrac{1}{4}\zeta^2 - \tfrac{3}{4}\beta s^2)\rho = 0 \tag{21}$$

whereas the equation obtained for s gives the solution

$$s = s_0 \exp(-\tfrac{1}{2}\varepsilon\zeta t) \tag{22}$$

In the case $|\zeta| \ll 1$, Eq. (21) describes an oscillator with a slowly varying frequency. Making the frequency 'frozen' enables one of the determining roots of the corresponding 'characteristic equation' to be obtained

$$k_{1,2} = \varepsilon\left(-\tfrac{1}{2}\zeta \pm \mathrm{i}\sqrt{\omega^2 - \tfrac{3}{4}\beta s^2}\right) \tag{23}$$

If the viscosity is negative, $\zeta < 0$, then Eqs. (21)–(23) qualitatively describe the transition to the local mode as the system energy increases. In particular, expression (23) shows that when the amplitude of the out-phase mode, which is associated with s, becomes large enough then the amplitude of the in-phase mode, ρ, loses its oscillatory character and grows monotonically.

As a result, one of the local mode increases its amplitude, whereas another one decays; see expressions (20). This is an onset of the dynamic transition to a localized mode. The corresponding critical time follows from explicit solution of Eqs. (22) and (23)

$$t^* = \frac{1}{\varepsilon|\zeta|}\ln\frac{4\omega^2}{3\beta s_0^2} \tag{24}$$

In order to provide numerical evidence for the dynamic transition from normal to local mode vibrations, let us introduce an indicator of the energy partition calculated as

$$P = \frac{E_1 - E_2}{E_1 + E_2} = \begin{cases} -1 & \text{if } E_1 = 0 \text{ and } E_2 \neq 0 \\ 0 & \text{if } E_1 = E_2 \\ 1 & \text{if } E_1 \neq 0 \text{ and } E_2 = 0 \end{cases} \tag{25}$$

where $E_i = (v_i^2 + \omega^2 u_i^2)/2$ is the total energy of i-th oscillator under the condition $\varepsilon = 0$.

Quantity (25) is varying within the interval $-1 \leqslant P \leqslant 1$. The ends of the interval obviously correspond to the local modes, whereas its center $P = 0$ corresponds to the normal modes.

The time history of the energy partition (25) is illustrated in Fig. 4. The following parameters were taken for numerical simulations: $\lambda = 0.05$, $\bar{\zeta} = -0.002$, $k = 1.0$, $\omega = \sqrt{2k + (17/2)\lambda^2} = 1.4217$, $\beta = 32/(9\varepsilon) = 383.29$,

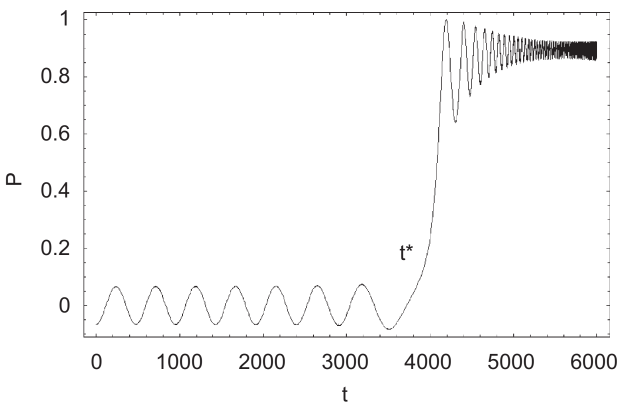

Fig. 4. 'Sudden' transition from normal to local mode vibration as the system energy has reached its critical value.

$\varepsilon = 15(\lambda/\omega)^2/2$, and therefore $\zeta = \bar{\zeta}/\varepsilon = -0.2156$. The initial normal mode amplitudes at zero velocities are $W_1(0) = 0.0001$ and $W_2(0) = -0.003$. The critical time estimate based on expression (24) $t^* = 3474.29$ is in quite a good match with Fig. 4.

4. Local mode interaction dynamics

Let us introduce new variables, K, θ and Δ, as follows:

$$\alpha_1 = \sqrt{K(t)}\cos\left[\frac{1}{2}\theta(t) + \frac{\pi}{4}\right]$$

$$\alpha_2 = \sqrt{K(t)}\sin\left[\frac{1}{2}\theta(t) + \frac{\pi}{4}\right] \tag{26}$$

$$\Delta = \delta_2 - \delta_1 + \pi \tag{27}$$

Further, considering the local mode total energies E_i under no interaction condition, and taking into account Eqs. (18), (26) and (28), gives

$$E_i = \tfrac{1}{2}(v_i^2 + \omega^2 u_i^2), \quad i = 1, 2 \tag{28}$$

$$E = E_1 + E_2 = \tfrac{1}{2}\omega^2(\alpha_1^2 + \alpha_2^2) = \tfrac{1}{2}\omega^2 K \tag{29}$$

$$\Delta E = E_1 - E_2 = \tfrac{1}{2}\omega^2(\alpha_1^2 - \alpha_2^2) = -\tfrac{1}{2}\omega^2 K \sin\theta \tag{30}$$

The variable K therefore is proportional to the total energy of the degenerated system, whereas the phase angle θ characterizes the energy partition between the local modes (25) as follows:

$$P = \frac{\Delta E}{E} = -\sin\theta \tag{31}$$

The third variable (27) describes the phase shift in the high-frequency vibrations between the local modes so that $\Delta = 0$ corresponds to the out-phase motions of the masses attached to the beam; note the difference with Eq. (20).

Differentiating Eqs. (27), (29) and (30), and enforcing Eq. (19), gives

$$\frac{d\kappa}{dt_1} = -\frac{\zeta}{\omega}\kappa$$

$$\frac{d\theta}{dt_1} = \sin\Delta$$

$$\frac{d\Delta}{dt_1} = -\cos\Delta\tan\theta + \kappa\sin\theta \tag{32}$$

where $t_1 = \varepsilon\omega t$ is a new temporal argument, and

$$\kappa = \frac{3\beta}{8\omega^2}K \tag{33}$$

In the conservative case, $\zeta = 0$, the first equation in Eq. (32) gives the energy integral $\kappa = \text{const.}$, whereas another two equations admit the integral

$$G = -\cos\Delta\cos\theta + \tfrac{1}{4}\kappa\cos 2\theta = \text{const.} \tag{34}$$

This particular case matches the results obtained for a linearly coupled set of Duffing's oscillators in Ref. [7], and later reproduced in Ref. [8], however, by means of different complex variable approaches. In particular, it was shown in Ref. [8] that the last two equations in Eq. (32) are equivalent to a strongly nonlinear conservative oscillator

$$\frac{d^2\theta}{dt_1^2} + G^2 \frac{\tan\theta}{\cos^2\theta} = 0 \tag{35}$$

as $\kappa \to 0$.

Oscillator (35) appears to be exactly solvable with general solution

$$\theta = \arcsin[\sin\theta_0 \sin(|G|t_1/\cos\theta_0)] \tag{36}$$

where θ_0 is the amplitude and another arbitrary constant can be introduced as a temporal shift.

Note that oscillator (35) was considered by Nesterov [9] as a phenomenological model for quite different kinds of problem. Since no direct physical meaning of such a unique 'restoring force characteristic' was found, the fact of exact solvability not attracted much attention for quite a long time.

In the case $\kappa \neq 0$, but still $\zeta = 0$, some perturbation occurs on the right-hand side of Eq. (35); the corresponding perturbation tool based on the action-angle variables was introduced in Ref. [8].

Let us show now that Eq. (32) can describe the transition to local modes under the assumption of small negative viscosity

$$|\zeta/\omega| \ll 1 \quad \text{and} \quad \zeta < 0 \tag{37}$$

Under condition (37), the factor κ in the third equation of Eq. (32) can be viewed as a slowly growing quasi-constant. In this case, making κ 'frozen' and linearizing the last two equations in Eq. (32) near the equilibrium $(\theta, \Delta) = (0, 0)$, gives

$$\frac{d^2\theta}{dt_1^2} + (1 - \kappa)\theta = 0 \tag{38}$$

Note that small θ and Δ bring the original system close to the out-of-phase vibration mode as follows from Eqs. (31) and (27). When the growing energy parameter κ passes the critical point $\kappa = 1$, the type of equilibrium is changing from a focus to a saddle point and thus the variable θ becomes exponentially growing. Practically, however, the exponential growth will be suppressed by the nonlinearity. As a result two limit phase trajectories (separatrix loops) occur around two new stable equilibrium points. These two points represent two new stable modes of the original system—local modes. The phase-plane diagrams for sub- and super-critical

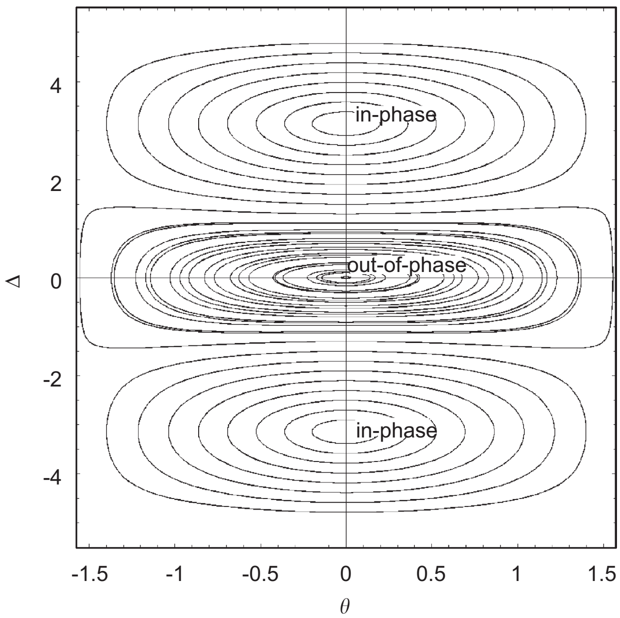

Fig. 5. Phase-plane structure at under-critical system energy, $\kappa = 0.5$.

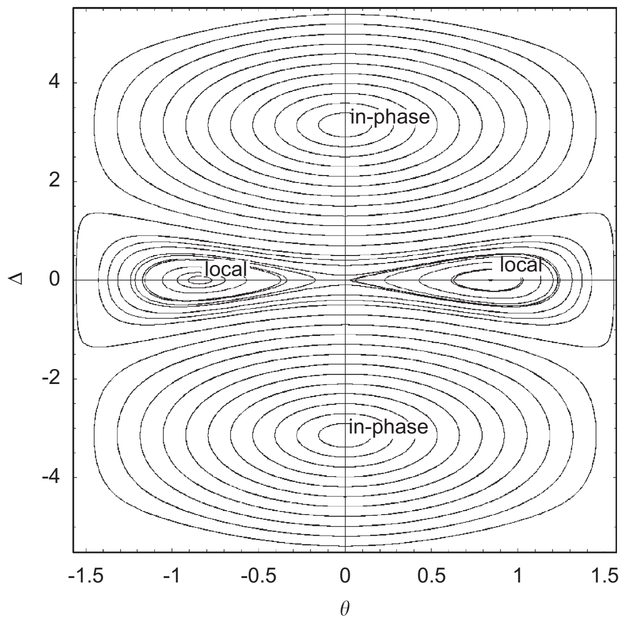

Fig. 6. Phase-plane structure at super-critical system energy, $\kappa = 1.5$.

energy levels are shown in Figs. 5 and 6, respectively. Note that the equilibrium subjected to such qualitative change corresponds to the out-of-phase vibration mode of the model, whereas another two equilibrium points, $(\theta, \Delta) = (0, \pm\pi)$, correspond to the same in-phase mode and remain stable. Therefore, out-of-phase vibrations appear to be less favorable to energy equipartition as the energy reaches its critical level. Note that links between localization and the presence of limit phase trajectories was discussed also in Ref. [7] based on the system of two coupled Duffing oscillators. In particular, the limit phase trajectories were interpreted as nonlinear beats of infinitely long period, keeping the energy near one of the two oscillators.

As follows from expression (31), the growth of θ increases the energy unbalance between the local modes, and that is onset of the mode localization. The corresponding critical time, at which the localization begins, is obtained from Eq. (33) as follows:

$$\frac{3\beta}{8\omega^2} K_0 \exp(\varepsilon|\zeta|t^*) = 1 \Longrightarrow t^* = \frac{1}{\varepsilon|\zeta|} \ln \frac{8\omega^2}{3\beta K_0} \tag{39}$$

As follows from Eqs. (20) and (29), $K_0 = 2(s_0^2 + \rho_0^2)$ therefore, under the condition $\rho_0^2 \ll 1$, expressions (24) and (39) give the same result.

5. Concluding remarks

In this paper, the phenomenon of dynamic transition from normal to local nonlinear modes was illustrated on a simply supported beam-spring model.

However, the developed analytical approach, describing the local mode interaction in terms of the energy and phase shift variables, appears to be independent of the individual features of the illustrating model and this can be used in other similar cases.

Compared to the previous publications [7,8] introducing the same set of descriptive variables, K, θ and Δ, current work has distinctive features as follows:

(1) Instead of general mass-spring models, an elastic beam supported by nonlinear springs is considered in this work. This provides clear interpretations for both the normal and local modes through the corresponding shape functions of the beam center line.

(2) Instead of using a quite complicated system reduction in terms of complex coordinates, it is shown that the same result can be achieved by means of a traditional set of amplitude-phase variables, and the standard one-frequency averaging procedure.
(3) The non-conservative case is considered in order to describe qualitative changes in the dynamics as the total energy of the system adiabatically increases or decreases. Based on such a generalization, new quantitative and qualitative results are obtained.

In particular, explicit expressions have been obtained for the critical time at which onset of the localization occurs. The phenomenon is explained in terms of the related phase-plane diagram subjected to a qualitative change (center-saddle transition) as the total energy of the system reaches its critical level.

References

[1] C. Jaffe, P. Brumer, Local and normal modes: a classical perspective, *The Journal of Chemical Physics* 73 (1980) 5646–5658.
[2] A.C. Scott, P.S. Lomdahl, J.C. Eilbeck, Between the local-mode and normal-mode limits, *Chemical Physics Letters* 113 (1985) 29–36.
[3] L.I. Manevich, V.N. Pilipchuk, Localization of oscillations in linear and nonlinear chains, *Advances in Mechanics* 13 (1990) 107–134 (in Russian).
[4] A.F. Vakakis, L.I. Manevitch, Y.V. Mikhlin, V.N. Pilipchuk, A.A. Zevin, *Normal Modes and Localization in Nonlinear Systems*, Wiley, New York, 1996.
[5] V.N. Pilipchuk, Transient mode localization in coupled strongly nonlinear exactly solvable oscillators, *Nonlinear Dynamics* 51 (2008) 245–258 ⟨http://dx.doi.org/10.1007/s11071-007-9207-4⟩.
[6] R.D. Richtmyer, *Principles of Advanced Mathematical Physics*, Vol. 1, Springer, Berlin, 1985.
[7] L.I. Manevich, New approach to beating phenomenon in coupled nonlinear oscillatory chains, *Archive of Applied Mechanics* 77 (2007) 301–312.
[8] V.N. Pilipchuk, Transitions from strongly to weakly-nonlinear dynamics in a class of exactly solvable oscillators and nonlinear beat phenomena, *Nonlinear Dynamics* 52 (4) (2008) 263–276 ⟨http://dx.doi.org/10.1007/s11071-007-9276-4⟩.
[9] S.V. Nesterov, Examples of nonlinear Klein–Gordon equations, solvable in terms of elementary functions, *Proceedings of Moscow Institute of Power Engineering* 357 (1978) 68–70.